Reaction Kinetics, Mechanisms and Catalysis
https://doi.org/10.1007/s11144-024-02673-3

Theoretical investigations of the reaction mechanism and kinetic for the reaction between mercury and hydrogen fluoride

Qinwei Yu[1] · Jianming Yang[1] · Hai-Rong Zhang[2] · Ge Gao[2] · Yongna Yuan[3] · Wei Dou[2] · Pan-Pan Zhou[2]

Received: 16 April 2024 / Accepted: 1 June 2024

Abstract

To understand the detailed reaction kinetics and mechanism of the reaction between Hg and HF, theoretical investigations of their reactions at different temperatures were carried out. The results suggest that the reactions goes through two steps. In the first step, Hg interacts with HF to form a complex HF···Hg, and then the F atom of HF approaches to Hg to form the transition state H•••F•••Hg, the bonding between F and Hg atoms results in the formation of HgF. Subsequently, the second HF molecule takes part in and it interacts with HgF to form the intermediate HF•••HgF, and then the transition state H•••F•••HgF forms due to the approaching of F atom of HF to Hg atom of HgF, finally the product HgF_2 is produced after the F and Hg atoms are bonded. The temperature significantly influences the reaction process. The weak interaction in the formation of the complex HF•••Hg as well as the intermediate HF•••HgF was illustrated by quantum theory of atoms in molecules (QTAIM). The kinetic parameters including the pre-exponential factor A, activation energy E_a and reaction rate k at different temperatures were calculated, and the expressions of reaction rates k for the reactions between HF and Hg to form HgF as well as HgF_2 were derived. The results would provide valuable insights into the chemical reaction of Hg and HF, the mechanism and the kinetics.

Keywords Hydrogen fluoride · Mercury · Weak interaction · Reaction mechanism · Kinetic investigation

✉ Pan-Pan Zhou
zhoupp@lzu.edu.cn

[1] State Key Laboratory of Fluorine and Nitrogen Chemicals, Xi'an Modern Chemistry Research Institute, Xi'an 710065, People's Republic of China

[2] Key Laboratory of Advanced Catalysis of Gansu Province, Advanced Catalysis Center, College of Chemistry and Chemical Engineering, Lanzhou University, 222 South Tianshui Road, Lanzhou 730000, People's Republic of China

[3] School of Information Science and Engineering, Lanzhou University, Lanzhou 730000, Gansu, People's Republic of China

Published online: 18 June 2024

Introduction

Mercury (Hg) is a volatile heavy metal pollutant [1] with trace amounts in coal [2], and it is one of the sources of global atmospheric pollutants which causes serious damage to the environment because the large amount of coal combustion releases mercury in the flue gas. Many efforts have been devoted to investigating the atmospheric chemistry of mercury and its transformation via the oxidation reactions of Hg(0) with reactive species [3]. For instance, Peterson and coworkers have systematically studied the reactions of Hg with a series of small halogen-containing molecules including Cl_2, Br_2, BrCl, ClO, BrO, I_2, IBr, ICl and IO [4–6]. Subsequently, they theoretically investigated the collision-induced dissociation and recombination of Hg and Br atoms [7]. Auzmendi-Murua and Bozzelli paid much attention on the emissions of gaseous Hg from combustion sources and their control [8], and they used a mechanism to explain the gas-phase Hg conversion in H_2, O_2, chloro C1-hydrocarbon, and NO_x combustion effluent. Then they reported that Hg present in the flue gas in coal burning can be oxidized by the addition of halogens (Cl, Br, I), and they proposed the detailed reaction mechanism and discussed the influence of different air–fuel equivalence ratios [9]. Wilcox and coworkers performed theoretical work in predicting rate constants for Hg oxidation reactions by hydrogen chloride and chloride [10–12], and for the decomposition of $HgCl_2$ [13] that may occur in the flue gases of coal combustion [14]. Dibble and coworkers also extensively explored the oxidation of Hg in the global atmosphere [15–20]. Saiz-Lopez et al. suggested that photoreduction of gaseous oxidized Hg(II) affects the global atmospheric Hg speciation, transport and deposition [21]. Different types of Mercury bonding were investigated by Cremer and coworkers, and their bond dissociation energies were reported which can provide useful data for the chemistry of Hg and reactions of elemental Hg in the atmosphere [22].

Besides Hg, the flue gas generated from coal combustion contains many compounds including the fluorine content [23, 24] due to the combustion of high fluorine-containing coals. Hydrogen fluoride (HF) can be generated during the thermal treatment of coals [25, 26] and it is an extremely toxic, corrosive gas at room temperature and normal pressure [27]. To know the fluorine gas species in flue gas, the pyrolysis of fluoroborate residue and proportions of three main fluorine gases (i.e., SiF_4, BF_3, and HF) at different temperatures was reported by Feng and coworkers [28], and they suggested that the content of HF increases continuously with the temperature, meaning that HF is an important form during coal processing F. Previous study showed that the halogen acids like HCl [29], HBr and HI have important effects on mercury conversion [2] and especially HBr and HI can oxidize more than 85% of the gas phase mercury at a low concentration of 2 ppm. The reactions of other species like chlorine [10], bromine [30], iodine [5], chlorine hydroxide [31], bromine hydroxide [5, 6], nitrogen oxides (NOx) and sulfur oxides (SOx) [9] with Hg would also occur and these reactions have also been studied. Therefore, the trace amount Hg could react with other components in the flue gas like HF. It stimulates our great interest in uncovering the influence of HF on the oxidation reaction of Hg and the detailed mechanism.

To shed light on the reaction processes of HF and Hg and the mechanism, we aim at using quantum chemical calculations to provide the information about the reactant, transition state, intermediate and product in the chemical reaction. It is shown that quantum chemical calculations are powerful in explaining the reaction mechanism [32]. Previously, several theoretical studies have been devoted to the reaction mechanism between mercury and chlorine containing gases or HF during coal combustion. For instance, Liu et al. theoretically investigated the reaction of hydrochloric acid (i.e., HCl) with Hg and elaborated the reaction mechanism [33]. Subsequently, Liu and co-workers investigated the reaction mechanism of Hg and HF during coal combustion and obtained the reaction kinetic parameters [34]. Gao and co-workers considered the effects of temperature and pressure on the Hg/HF reaction in coal combustion [35]. Noticeably, in these previous studies, they did not considered the initial reaction of HF (or HCl) and Hg to form the complex of HF•••Hg (or HCl•••Hg) because the strong electronegativity of F (or Cl) atom. Accordingly, in the present work, quantum chemical calculations were employed to thoroughly explore the oxidation reaction processes of Hg by HF and the reaction mechanism, the geometries of the transition states and intermediates in the reaction processes will be discussed, the detailed mechanism and the kinetics of the reactions will be illustrated.

Computational details

The geometric structures of Hg, HF, transition state, intermediate and product were optimized using the M06-L functional [36, 37] corrected with the Grimme's dispersion (D3) [38] because of the importance of dispersion interaction in weak interaction system [39–41], and the 6–311 + + G(2d,2p) basis set was used for the H and F atoms while the Hg atom was treated using the relativistic ECP60MDF pseudopotential of the Stuttgart group [42] together with cc-pwCVnZ-PP [43] valence basis set. The counterpoise method proposed by Boys and Bernardi [44] was used to consider the basis set superposition error (BSSE) for the complex formed in the reaction. Vibrational frequency calculations were conducted at the same level of theory to ensure that the optimized reactants, intermediates and product have no imaginary frequencies while the transition state has only one imaginary frequency. Intrinsic reaction coordinate (IRC) [45] calculations at the above level of theory were carried out to confirm that the transition state obtained was true. All the calculations were performed via the Gaussian16 program [46]. Quantum theory of atoms in molecules (QTAIM [47–49]) was employed to analyze the bond critical points (BCPs) in the complex and intermediate using the Multiwfn software [50]. The relative Gibbs free energy (i.e., ΔG) is calculated as the difference between the Gibbs free energy of the complex (or the transition state or intermediate or product) and the sum of Gibbs free energies of the reactants. The interaction energy (i.e., ΔE) of the complex is calculated as the energy difference between the total energy of the complex (or the intermediate) and the sum of energies of its components. The interaction energy of the complex after considering BSSE is termed as ΔE_{corr}, which is calculated as the sum of ΔE and E_{BSSE} (i.e., $\Delta E_{\mathrm{corr}} = \Delta E + E_{\mathrm{BSSE}}$).

The reaction occurs between Hg and HF at the different temperatures from room temperature to 1000 K was investigated, which involves the following reactions (i.e., reaction formulas Eqs. 1 and 2):

$$HF + Hg \rightarrow H + HgF \tag{1}$$

$$HF + HgF \rightarrow H + HgF_2 \tag{2}$$

In terms of transition state theory, the parameters including the reaction rate constant k, pre-exponential factor A and activation energy E_a were calculated to understand the reaction tendency.

$$k = AT^n e^{\left(-\frac{E_a}{RT}\right)} \tag{3}$$

$$A = \frac{k_B T}{h} \frac{Q^{\neq}}{\Pi Q_B} \tag{4}$$

For Eqs. 3 and 4, n is the temperature index, R is the gas constant, T is the temperature, k_B is Boltzmann's constant, h is Planck's constant, $Q^{\neq}$ is the partition function of the transition state, ΠQ_B is the continued product of the partition functions (Q_B) of all reaction species B. The KiSThelP [51] software was used for the data processing and analysis in obtaining the reaction rate constant k and pre-exponential factor A.

Results and discussion

The reaction between Hg and HF first goes through the reaction formula (Eq. 1), the oxidation of Hg by one HF molecule enables Hg to react with F atom of HF as HgF, and then HgF reacts with the other HF molecule to form HgF_2 via the reaction formula (Eq. 2). The calculated results show that the oxidation reaction between Hg and HF goes through an intermediate in which HF interacts with Hg to form a complex HF•••Hg, and then a transition state H•••F•••Hg forms due to the broken of H–F bond, the further approaching of F atom to Hg atom results in the bonding between F and Hg atom, so the processes can be represented as:$HF + Hg \rightarrow HF \bullet\bullet\bullet Hg \rightarrow H \bullet\bullet\bullet F \bullet\bullet\bullet Hg \rightarrow H + HgF$. The subsequent reaction between HgF and the other HF molecule undergoes the formations of the intermediate HF•••HgF, the transition state H•••F•••HgF and the final product HgF_2, so it can be represented as: $HF + HgF \rightarrow HF \bullet\bullet\bullet HgF \rightarrow H \bullet\bullet\bullet F \bullet\bullet\bullet HgF \rightarrow H + HgF_2$. Herein the reaction processes occur at 298 K and the effect of the temperature from 298 to 1000 K on the reaction were explored and discussed in detailed.

With regard to the reaction between Hg and HF at each temperature (298–1000 K), the Gibbs free energy profiles was depicted in Figs. 1 and S1, and the optimized structures of the complex, transition state and intermediate were depicted in Fig. 2. It can be seen that both the complex HF•••Hg and the transition state H•••F•••Hg form in the reaction of Hg and HF at each temperature, and it is

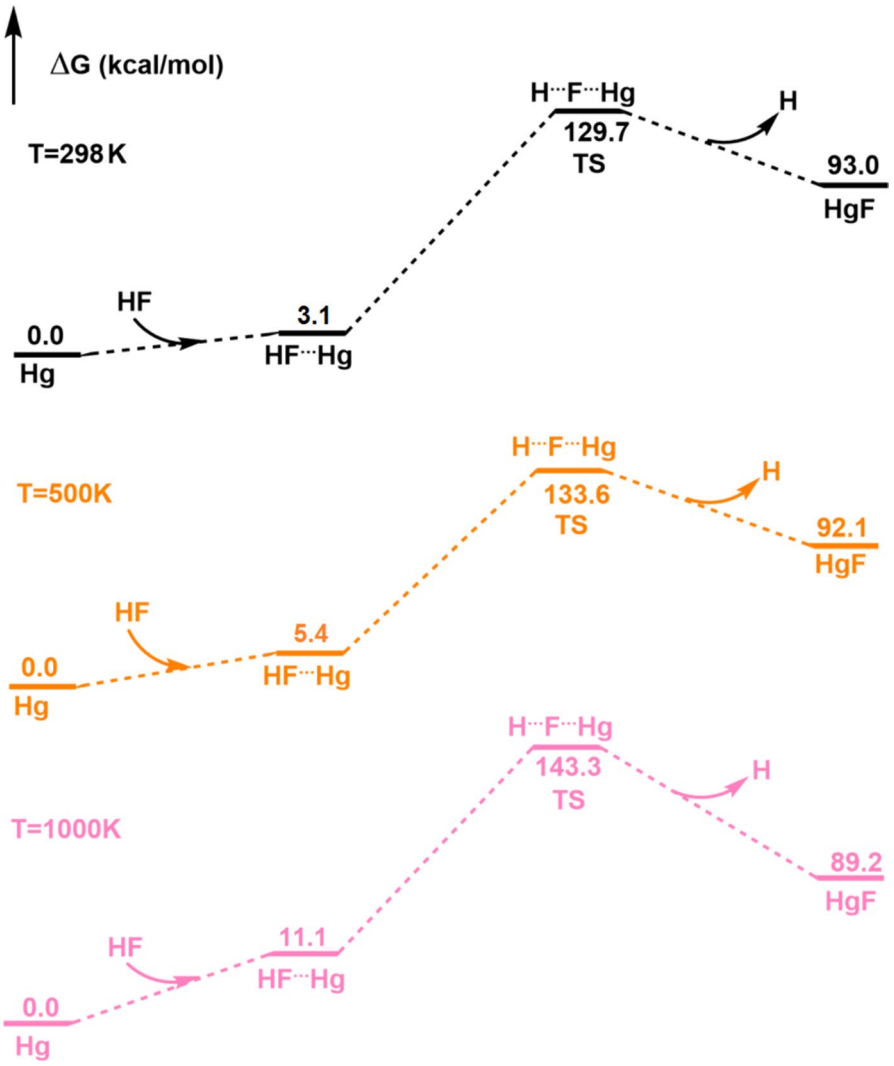

Fig. 1 Gibbs free energy profiles for the reactions of Hg and HF at 298 K, 500 K and 1000 K

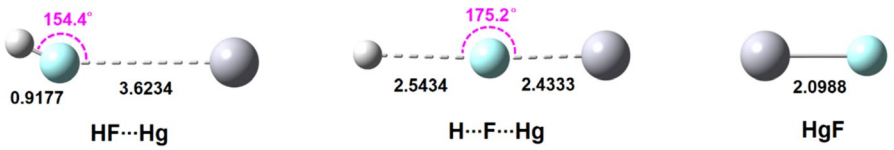

Fig. 2 The optimized structures of the complex, transition state and intermediate for the reaction of Hg and HF (The units of distances and bond angles are in Å and degree)

different from the previous result in which only one transition state but not any intermediate was observed [34, 35]. The interaction energy (i.e., ΔE_1) between HF and Hg for the complex HF•••Hg is − 0.46 kcal/mol or − 0.37 kcal/mol after considering BSSE at each temperature, meaning the formation of weak interaction between HF and Hg before the oxidation reaction. QTAIM analysis shows that the electron density (i.e., ρ) and its Laplacian (i.e., $\nabla^2\rho$) at the BCP of F•••Hg interaction are 0.0032 and 0.0136 a.u., respectively. These values are out of the ranges of the criteria for the existence of hydrogen bond (i.e., ρ and $\nabla^2\rho$ should be within the ranges of 0.002–0.035 and 0.024–0.139 a.u., respectively [52]). The result indicates that the F•••Hg interaction in the complex HF•••Hg is van der Waals interaction. The positive (or negative) electronic energy density (i.e., H) value at the BCP is indicative of electrostatic (or covalent) dominant interaction [53], so the positive H value ($H = 0.0007$ a.u.) for F•••Hg interaction in the complex HF•••Hg suggests it is of mainly electrostatic character. To form the complex HF•••Hg, it needs to absorb an energy ranging from 3.1 to 11.1 kcal/mol, while the energy barrier for the conversion from the complex HF•••Hg to the transition state H•••F•••Hg is in the range of 126.6–132.2 kcal/mol, which is decreased with the increase of the temperature (Fig. 1). It is found that the geometries of the reactant, complex, transition state, intermediate and product are not influenced by the temperature. At each temperature (298–1000 K), the H–F bond length and F•••Hg distance in the complex HF•••Hg are 0.9177 and 3.6234 Å (Fig. 2), respectively. The elongated H-F bond length in the complex HF•••Hg relative to that in HF molecule at each temperature should be ascribed to the formation of F•••Hg weak interaction. It is observed that the H•••F distance in the transition state (i.e., TS) H•••F•••Hg is 2.5434 Å (Fig. 2), suggesting that the H-F bond is broken. As a result, the intermediate HgF is produced.

Subsequently, HgF interacts with the other HF molecule to form the intermediate HF•••HgF, which is not observed in the previous work [34, 35]. The interaction energy (i.e., ΔE_2) between HF and HgF for the intermediate HF•••HgF is − 1.93 kcal/mol or − 1.75 kcal/mol after considering BSSE, meaning that HF can interact with HgF through weak attractive interaction. The electron density ρ and its Laplacian $\nabla^2\rho$ at the BCP of F•••Hg interaction in the intermediate HF•••HgF from QTAIM analysis are 0.0086 and 0.0304 a.u., respectively. Obviously, these values within the ranges of the criteria for the existence of hydrogen bond, and they are even larger than 0.002 and 0.024 a.u., respectively. It suggests that the F•••Hg interaction in the intermediate HF•••HgF is a strong attractive interaction. The electronic energy density (i.e., H) at the BCP of F•••Hg interaction in the intermediate HF•••HgF is 0.0006 a.u., meaning the F•••Hg interaction is of mainly electrostatic character. The process in the formation of the intermediate HF•••HgF needs to absorb an energy in the range of 3.4–13.5 kcal/mol from 298 to 1000 K (Figs. 3 and S2). Then the F atom of HF in the intermediate HF•••HgF approaches to HgF, resulting in the formation of the transition state (i.e., TS) H•••F•••HgF. The process from HF•••HgF to H•••F•••HgF needs to overcome an energy barrier ranging from 47.0 to 57.5 kcal/mol from 298 to 1000 K (Fig. 3). In the intermediate HF•••HgF, the F•••Hg distance is 3.1521 Å, while the H–F and Hg–F bond lengths are 0.9193 and 2.1038 Å, respectively (Fig. 4). In the transition state H•••F•••HgF, the H•••F and F•••Hg distances are 1.3500 and 2.2801 Å, respectively. Due to the bonding

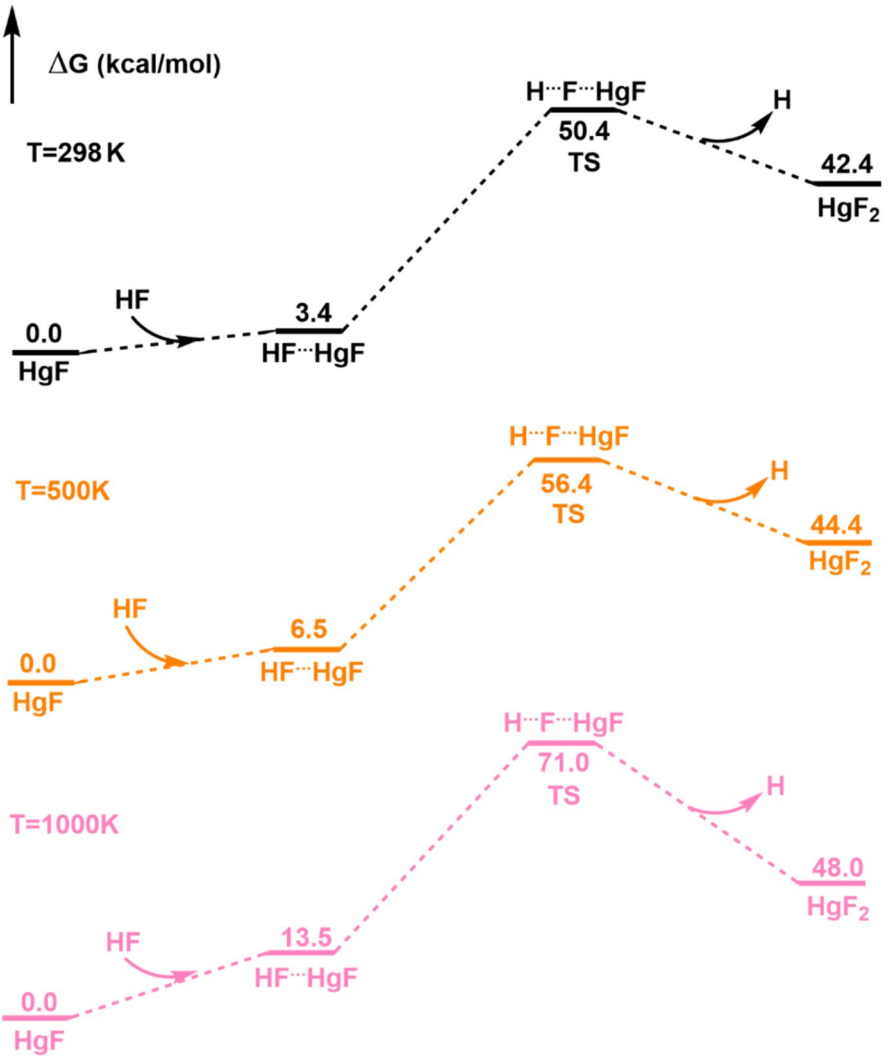

Fig. 3 Gibbs free energy profiles for the reactions of HF and HgF at 298 K, 500 K and 1000 K

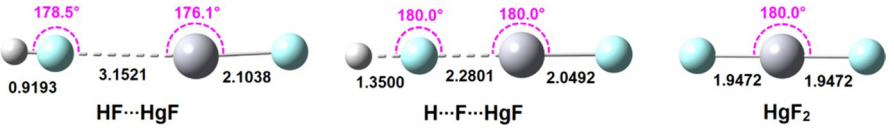

Fig. 4 The optimized structures of the intermediate, transition state and product for the reaction of HF and HgF (The units of distances and bond angles are in Å and degree)

between F and Hg atoms, the final product HgF_2 is yielded. The Hg-F bond in HgF_2 (ca. 1.9472 Å) is shorter than that in the intermediate HgF (i.e., 2.0988 Å).

In terms of the above calculations, the kinetic parameters for the reactions between HF and Hg to form HgF (i.e., the reaction occurring in the form of formula (Eq. 1)) and then HgF_2 (i.e., the reaction occurring in the form of formula (Eq. 2)) at different temperatures were calculated using the KiSThelP software. As outlined in Table 1, the reaction rate constant k gradually increases with the rise of the temperature for the reaction between HF and Hg in the formation of HgF. For the reactions between HF and HgF to form HgF_2, it can be seen from Table 2 that the pre-exponential factor A varies slightly with the rise of the temperature, and the reaction rate constant k gradually increases with the rise of the temperature. To obtain the expression of reaction rate, the relationship between $\log_{10}k$ and $10^3/T$ is explored. As depicted in Fig. 5a and b, the linear relationship between $\log_{10}k$ and $10^3/T$ is observed, and the fitting reaction kinetic parameters including pre-exponential factor A and activation energy E_a can be derived which are summarized in Table 3. Consequently, the expression of reaction rate k can be written as well, as shown in Table 3. It is expected that these kinetic parameters would be helpful for the investigation of the reaction involving Hg and other gas in flue gas.

Conclusions

In this work, the reactions of Hg with hydrogen fluoride (HF) at different temperatures were theoretically investigated and the detailed mechanisms were explored, and the results indicate that the reactions can be divided into two steps. In the step one, Hg was firstly oxidized by one HF molecule and forms HgF. In this reaction

Table 1 Kinetic parameters (A, unit in $cm^3\ mol^{-1}\ s^{-1}$; E_a, unit in kJ mol^{-1}; k, unit in $cm^3\ mol^{-1}\ s^{-1}$) for the reactions between HF and Hg to form HgF at different temperatures (T, unit in K)

T	A	E_a	k
298	6.28×10^{12}	522.65	7.72×10^{-81}
300	6.32×10^{12}	522.66	3.15×10^{-80}
350	7.37×10^{12}	522.98	3.24×10^{-67}
400	8.41×10^{12}	523.31	1.89×10^{-57}
450	9.45×10^{12}	523.66	7.53×10^{-50}
500	1.05×10^{13}	524.02	9.15×10^{-44}
550	1.15×10^{13}	524.39	8.77×10^{-39}
600	1.26×10^{13}	524.76	1.25×10^{-34}
650	1.36×10^{13}	525.14	4.13×10^{-31}
700	1.47×10^{13}	525.52	4.30×10^{-28}
750	1.57×10^{13}	525.90	1.78×10^{-25}
800	1.67×10^{13}	526.27	3.49×10^{-23}
850	1.78×10^{13}	526.65	3.68×10^{-21}
900	1.88×10^{13}	527.02	2.32×10^{-19}
950	1.99×10^{13}	527.39	9.51×10^{-18}
1000	2.09×10^{13}	527.75	2.69×10^{-16}

Table 2 Kinetic parameters (A, unit in $cm^3\ mol^{-1}\ s^{-1}$; E_a, unit in $kJ\ mol^{-1}$; k, unit in $cm^3\ mol^{-1}\ s^{-1}$) for the reactions between HF and HgF to form HgF_2 at different temperatures (T, unit in K)

T	A	E_a	k
298	6.24×10^{12}	181.48	2.07×10^{-22}
300	6.28×10^{12}	181.47	3.38×10^{-22}
350	7.32×10^{12}	181.45	1.11×10^{-17}
400	8.36×10^{12}	181.53	2.70×10^{-14}
450	9.41×10^{12}	181.68	9.28×10^{-12}
500	1.04×10^{13}	181.90	1.51×10^{-9}
550	1.15×10^{13}	182.17	1.12×10^{-7}
600	1.25×10^{13}	182.49	1.79×10^{-6}
650	1.36×10^{13}	182.84	3.78×10^{-5}
700	1.46×10^{13}	183.22	4.26×10^{-4}
750	1.57×10^{13}	183.63	2.78×10^{-3}
800	1.67×10^{13}	184.05	2.21×10^{-2}
850	1.77×10^{13}	184.49	8.98×10^{-2}
900	1.88×10^{13}	184.94	4.83×10^{-1}
950	1.98×10^{13}	185.39	1.78
1000	2.09×10^{13}	185.85	5.78

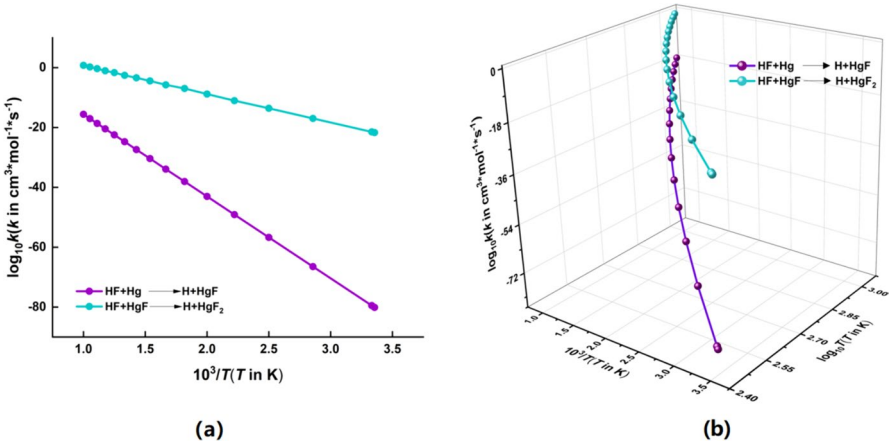

Fig. 5 The relationships **a** between $\log_{10}k$ and $10^3/T$ and **b** among $\log_{10}k$, $10^3/T$ and and $\log_{10}T$ for the reaction between HF and Hg to form HgF and then HgF_2

Table 3 Fitting reaction kinetic parameters (A, unit in $cm^3\ mol^{-1}\ s^{-1}$; n, dimensionless constant; E_a, unit in $kJ\ mol^{-1}$) for the reactions between HF and Hg to form HgF and then HgF_2, and the expression of reaction rate (k, unit in $cm^3\ mol^{-1}\ s^{-1}$)

Reaction	A	n	E_a	k
$HF+Hg\rightarrow H+HgF$	8.29×10^{8}	0.9024	520.6	$k=8.29\times10^{8}T^{0.9024}e^{-62617.27/T}$
$HF+HgF\rightarrow H+HgF_2$	6.68×10^{7}	0.7518	178.9	$k=6.68\times10^{7}T^{0.7518}e^{-21521.31/T}$

processes, Hg first interacts with HF to form a complex HF•••Hg, and then the approaching of F atom of HF to Hg leads to a transition state H•••F•••Hg which is accompanied by the broken of H–F bond, and subsequently, the bonding between F and Hg atom causes the formation of HgF. Afterwards the other HF molecule takes part in and reacts with HgF to form HgF_2. In this step, HgF and the other HF molecule first interacts with each other to form the intermediate HF•••HgF, and then the approaching of F atom of HF to Hg atom of HgF results in the transition state H•••F•••HgF, and the final product HgF_2 is produced due to the bond formed between F and Hg atom. The temperature has a significant effect on the reaction process but has little effect on the geometries of the reactant, complex, intermediate, transition state and product. Based on the above results, we further calculated the kinetic parameters including the pre-exponential factor A, activation energy E_a and reaction rate k at different temperatures, and the linear fitting further provides us the expressions of reaction rates k for the reactions between HF and Hg to form HgF and then HgF_2. The results presented here would be insightful into the understanding of the chemical reactions of Hg and HF, the mechanisms and the kinetics.

Supplementary Information The online version contains supplementary material available at https://doi.org/10.1007/s11144-024-02673-3.

Acknowledgements We acknowledge the financial supports of the Open and Cooperation Innovation Fund from Xi'an Modern Chemistry Research Institute and the Fundamental Research Funds for the Central Universities under Grant No. lzujbky-2021-sp43.

Funding Funding was provided by Fundamental Research Funds for the Central Universities (Grant No. lzujbky-2021-sp43).

Data availability The data that support the findings of this study are available in the electronic supplementary material (in part) or from the corresponding author upon reasonable request (in whole).

Declarations

Conflict of interest The authors declare that they have no conflict of interest.

References

1. Pacyna EG, Pacyna JM, Steenhuisen F, Wilson S (2006) Global anthropogenic mercury emission inventory for 2000. Atmos Environ 40:4048–4063
2. Eswaran S, Stenger HG (2008) Effect of halogens on mercury conversion in SCR catalysts. Fuel Process Technol 89:1153–1159
3. Li Z, Sun Y, Yin Y, Liang Y, Cai Y (2022) Advances in computational chemistry for oxidation and reduction of mercury in the atmosphere. Environ Chem 41:83–93
4. Balabanov NB, Peterson KA (2003) Mercury and reactive halogens: the thermochemistry of Hg + {Cl_2, Br_2, BrCl, ClO, and BrO}. J Phys Chem A 107:7465–7470
5. Shepler BC, Balabanov NB, Peterson KA (2005) Ab initio thermochemistry involving heavy atoms: an investigation of the reactions Hg + IX (X= I, Br, Cl, O). J Phys Chem A 109:10363–10372
6. Shepler BC, Peterson KA (2003) Mercury monoxide: a systematic investigation of its ground electronic state. J Phys Chem A 107:1783–1787
7. Shepler BC, Balabanov NB, Peterson KA (2007) Hg+Br->HgBr recombination and collision-induced dissociation dynamics. J Chem Phys 127:164304

8. Auzmendi-Murua I, Bozzelli JW (2010) Gas-phase mercury conversion in H2, O2, chloro C1-hydrocarbon, and NOx combustion effluent from use of an elementary kinetic mechanism. Combust Sci Technol 182:529–543
9. Auzmendi-Murua I, Bozzelli JW (2016) Gas phase mercury oxidation by halogens (Cl, Br, I) in combustion effluents: influence of operating conditions. Energy Fuels 30:603–615
10. Wilcox J (2009) A kinetic investigation of high-temperature mercury oxidation by chlorine. J Phys Chem A 113:6633–6639
11. Wilcox J (2011) A kinetic investigation of unimolecular reactions involving trace metals at post-combustion flue gas conditions. Environ Chem 8:207–212
12. Wilcox J, Robles J, Marsden DCJ, Blowers P (2003) Theoretically predicted rate constants for mercury oxidation by hydrogen chloride in coal combustion flue gases. Environ Sci Technol 37:4199–4202
13. Wilcox J, Blowers P (2004) Decomposition of mercuric chloride and application to combustion flue gases. Environ Chem 1:166–171
14. Wilcox J, Marsden DCJ, Blowers P (2004) Evaluation of basis sets and theoretical methods for estimating rate constants of mercury oxidation reactions involving chlorine. Fuel Process Technol 85:391–400
15. Dibble TS, Tetu HL, Jiao Y, Thackray CP, Jacob DJ (2020) Modeling the OH-initiated oxidation of mercury in the global atmosphere without violating physical laws. J Phys Chem A 124:444–453
16. Dibble TS, Zelie MJ, Jiao Y (2014) Quantum chemistry guide to PTRMS studies of As-yet undetected products of the bromine-atom initiated oxidation of gaseous elemental mercury. J Phys Chem A 118:7847–7854
17. Horowitz HM, Jacob DJ, Zhang Y, Dibble TS, Slemr F, Amos HM et al (2017) A new mechanism for atmospheric mercury redox chemistry: implications for the global mercury budget. Atmos Chem Phys 17:6353–6371
18. Jiao Y, Dibble TS (2017) Structures, vibrational frequencies, and bond energies of the BrHgOX and BrHgXO species formed in atmospheric mercury depletion events. J Phys Chem A 17:6353–6371
19. Lam KT, Wilhelmsen CJ, Dibble TS (2019) BrHgO• + C2H4 and BrHgO• + HCHO in atmospheric oxidation of mercury: determining rate constants of reactions with pre-reactive complexes and a bifurcation. J Phys Chem A 123:6045–6055
20. Shah V, Jacob DJ, Thackray CP, Wang X, Sunderland EM, Dibble TS et al (2021) Improved mechanistic model of the atmospheric redox chemistry of mercury. Environ Sci Technol 55:14445–14456
21. Saiz-Lopez A, Sitkiewicz SP, Roca-Sanjuán D, Oliva-Enrich JM, Dávalos JZ, Notario R et al (2018) Photoreduction of gaseous oxidized mercury changes global atmospheric mercury speciation, transport and deposition. Nat Commun 9:4796
22. Cremer D, Kraka E, Filatov M (2008) Bonding in mercury molecules described by the normalized elimination of the small component and coupled cluster theory. ChemPhysChem 9:2510–2521
23. Luo K (2005) Arsenic content and distribution pattern in Chinese coals. J Toxicol Environ Health Part B 87:427–438
24. Zhao C, Luo K (2017) Sulfur, arsenic, fluorine and mercury emissions resulting from coal-washing byproducts: a critical component of China's emission inventory. Atmos Environ 152:270–278
25. Guo S, Yang J, Liu Z (2006) The fate of fluorine and chlorine during thermal treatment of coals. Environ Sci Technol 40:7886–7889
26. Qi Q, Liu J, Cao X, Zhou J, Cen K (2002) Fluorine distribution characteristics in coal and behavior of fluorine during coal combustion. J Chem Ind Eng 53:572–577
27. Jang HJ, Kim RH, Kwon HS, Kim TS, Lee JH (2009) Study on corrosion resistance of gas cylinder materials in HF, HCl and HBr environments. Corrosion Eng Sci Technol 44:445–452
28. Feng Y, Jiang X, Chi Y, Li X, Zhu H (2012) Volatilization behavior of fluorine in fluoroborate residue during pyrolysis. Environ Sci Technol 46:307–311
29. Sliger RN, Kramlich JC, Marinov NM (2000) Towards the development of a chemical kinetic model for the homogeneous oxidation of mercury by chlorine species. Fuel Process Technol 65–66:423–438
30. Wilcox J, Okano T (2011) Ab initio-based mercury oxidation kinetics via bromine at postcombustion flue gas conditions. Energy Fuel 25:1348–1356
31. Khalizov AF, Viswanathan B, Larregaray P, Ariya PA (2003) A Theoretical study on the reactions of Hg with halogens: atmospheric implications. J Phys Chem A 107:6360–6365
32. Roduner E (2014) Understanding catalysis. Chem Soc Rev 43:8226–8239

33. Liu J, Wang MH, Zheng CG, Xu MH, Li LC, Xu JY (2003) Reaction mechanism of mercury and gases during coal combustion. J Eng Thermophys 24:161–164
34. Liu J, Wang SC, Liu Y, Zheng CG (2011) Reaction mechanism of mercury and HF during coal combustion. J Eng Thermophys 32:695–698
35. Gao Z, Chen S, Wu P, Li J, Yin L, Chen C (2014) Kinetic study on Hg/HF reaction in coal combustion. Thermal Power Gen 43:96–101
36. Zhao Y, Truhlar DG (2006) A new local density functional for main-group thermochemistry, transition metal bonding, thermochemical kinetics, and noncovalent interactions. J Chem Phys 125:194101
37. Zhao Y, Truhlar DG (2008) The M06 suite of density functionals for main group thermochemistry, thermochemical kinetics, noncovalent interactions, excited states, and transition elements: two new functionals and systematic testing of four M06-class functionals and 12 other functionals. Theor Chem Acc 120:215–241
38. Grimme S, Antony J, Ehrlich S, Krieg H (2010) A consistent and accurate ab initio parametrization of density functional dispersion correction (DFT-D) for the 94 elements H-Pu. J Chem Phys 132:154104
39. Hadipour NL, Peyghan AA, Soleymanabadi H (2015) Theoretical study on the Al-Doped ZnO nanoclusters for CO chemical sensors. J Phys Chem C 119:6398–6404
40. Jameh-Bozorghi S, Soleymanabadi H (2017) Warped $C_{80}H_{30}$ nanographene as a chemical sensor for CO gas: DFT studies. Phys Lett A 381:646–651
41. Zhang M, Li B, Chen Y, Zhang J, Zhang Y, Song H, Soleymanabadi H, Wu J (2024) Theoretical approach on Hg^{2+}, Pb^{2+} and Cd^{2+} ions adsorption via phographene. J Ind Eng Chem 132:572–577
42. Figgen D, Rauhut G, Dolg M, Stoll H (2005) Energy-consistent pseudopotentials for group 11 and 12 atoms: adjustment to multiconfiguration Dirac–Hartree–Fock data. Chem Phys 311:227–244
43. Peterson KA, Puzzarini C (2005) Systematically convergent basis sets for transition metals. II. Pseudopotential-based correlation consistent basis sets for the group 11 (Cu, Ag, Au) and 12 (Zn, Cd, Hg) elements. Theor Chem Acc 114:283
44. Boys SF, Bernardi F (1970) The calculation of small molecular interactions by the differences of separate total energies. Some procedures with reduced errors. Mol Phys 19:553–566
45. Fukui K (1981) The path of chemical reactions: the IRC approach. Acc Chem Res 14:363–368
46. Frisch MJ, Trucks GW, Schlegel HB, Scuseria GE, Robb MA, Cheeseman JR et al (2016) Gaussian 16, Revision A.03. Gaussian Inc, Wallingford
47. Bader RFW (1985) Atoms in molecules. Acc Chem Res 18:9–15
48. Bader RFW (1990) Atoms in molecules: a quantum theory. Oxford University Press, Oxford
49. Bader RFW (1991) A Quantum theory of molecular structure and its applications. Chem Rev 91:893–928
50. Lu T, Chen F (2012) Multiwfn: a multifunctional wavefunction analyzer. J Comput Chem 33:580–592
51. Canneaux S, Bohr F, Henon E (2014) KiSThelP: a program to predict thermodynamic properties and rate constants from quantum chemistry results. J Comput Chem 35:82–93
52. Lipkowski P, Grabowski SJ, Robinson TL, Leszczynski J (2004) Properties of the C–H···H dihydrogen bond: an ab initio and topological analysis. J Phys Chem A 108:10865–10872
53. Arnold WD, Oldfied E (2000) The chemical nature of hydrogen bonding in proteins via NMR: J-couplings, chemical shifts, and AIM theory. J Am Chem Soc 122:12835–12841